# Mitigation of lateral slope movement and soil improvement using the vacuum-PVD scheme

S. Soralump[1], N. Koirala[2] and S. Phakdimek[3]

[1]*Associate Professor, Department of Civil Engineering, Faculty of Engineering, Kasetsart University, Bangkok, Thailand, E-mail: soralump_s@yahoo.com (corresponding author) (Orcid:0000-0001-7446-1860)*
[2]*Graduate Research student, Department of Civil Engineering, Faculty of Engineering, Kasetsart University, Bangkok, Thailand, E-mail: nishkarsha.koirala8@gmail.com (Orcid:0000-0002-8274-3179)*
[3]*Researcher, Geotechnical Engineering Research and Development Centre (GERD), Kasetsart University, Bangkok, Thailand, E-mail: sartsin.p@gmail.com (Orcid:0000-0001-5008-5282)*

Received 11 January 2022, accepted 11 September 2022

ABSTRACT: This paper interprets the results from field monitoring which was carried out during vacuum-PVD improvement in a site located near an actively moving slope. Interestingly, the monitoring results showed, among other things, mitigation in the outward lateral movements during and after the preloading process indicating relative stability in the slope and the efficiency of vacuum to mitigate lateral movements during the preloading period. Analyses were made on other field parameters such as pore pressure and settlement, as well as back-calculation of flow parameters to be considered during vacuum preloading design, such as permeability ratio ($k_h/k_s$) and horizontal consolidation coefficient ($C_h$) due to vacuum-PVD, were carried out. Post improvement, appropriate geotechnical properties were obtained from laboratory tests of clay specimens from borehole samples and undrained shear strengths were measured from unconfined compression and field vane shear test. The obtained properties indicated improvement in soft soil properties with a reduction in water content and an increase in maximum past pressure, OCR and undrained shear strengths. The prediction made for final shear strength using past literature, where applied additional incremental stress was reduced with depth, matched well with the shear strengths recorded from field testing.

KEYWORDS: Geosynthetics, soft clay, ground improvement, field testing & monitoring, slope movement

REFERENCE: Soralump, S., Koirala, N. and Phakdimek, S. (2022). Mitigation of lateral slope movement and soil improvement using the vacuum-PVD scheme. *Geosynthetics International*. [https://doi.org/10.1680/jgein.22.00003]

## 1. INTRODUCTION

The development of infrastructure in Bangkok continues at an unprecedented rate. The presence of soft clay layer in Bangkok makes it difficult to utilize available land without substantially improving its properties. Since soft clays have low shear strength, high compressibility and are sensitive to changes in water content compared to other soils, there can be settlement problems if construction works are carried out without suitable measures. The use of conventional prefabricated vertical drains (PVD), originally proposed by Kjellman (1952), with surcharge preloading, is one of the widely-used techniques because of its ability to reduce the consolidation time by shortening the drainage path and providing a better flow of water to permeable drainage layers (Hansbo 1979, 1981; Bergado *et al.* 1996, 2002; Abuel-Naga *et al.* 2015). Nowadays, vacuum-PVD is preferred as it is a faster soft ground improvement method, besides being environmentally friendly and cost-efficient. (Chu *et al.* 2000; Indraratna *et al.* 2005, 2010 2012; Chai *et al.* 2006, 2008 2013, 2020, 2021; Saowapakpiboon *et al.* 2009, 2010a 2010b; Shuwang *et al.* 2009; Lam *et al.* 2015; Long *et al.* 2015, 2016; Fang *et al.* 2019; Lei *et al.* 2019; Ni *et al.* 2019; Wang *et al.* 2019; Anda *et al.* 2020; Bergado *et al.* 2020; Hayashi *et al.* 2021; Zhang *et al.* 2021) including clogging effects (Cai *et al.* 2018; Deng *et al.* 2019; Wang *et al.* 2020; Xu *et al.* 2020; Zhou *et al.* 2021).

Many case studies on the application of the vacuum consolidation method (VCM) have been published, mostly concerning the improvement of naturally deposited soft clays. Some of the backfilled and reclaimed areas have also utilized the VCM soil improvement method (Bergado *et al.* 1998; Choa *et al.* 2001; Bergado *et al.*

2002, 2021 2022; Long *et al*. 2013; Alditra *et al*. 2020; Phakdimek *et al*. 2020; Wu *et al*. 2020). It has been shown that soft clays can be successfully improved by the application of vacuum pressure in conjunction with PVD. Even with a lesser amount of surcharge, the preloading time can be reduced and the undrained shear strength of soil can be increased by 1.5 to 2 times. Some of the case studies reporting the use of VCM even showed that the increase in undrained shear strength could be as high as 2 to 4 times (Bergado *et al*. 1998; Shang *et al*. 1998; Chu *et al*. 2006). Even though the use of VCM with surcharge has been demonstrated to be effective, its use may not always be feasible. The application of surcharge increases the total stress and the soil may be too weak to bear the applied load, causing significant outward lateral movement in the adjacent area. Such deformations have also been previously reported (Tavenas *et al*. 1974; Qi *et al*. 2020). In contrast, vacuum pressure alone induces inward lateral deformation and isotropic consolidation, so both types of deformations (outward or inward) are expected during vacuum preloading (with or without surcharge). The outward lateral deformations during preloading by surcharge and vacuum combination are also dependent on the magnitude of vertical settlement in the soils and under large loading, there may be significant vertical settlement causing substantial lateral deformation (Zhang *et al*. 2021). Under the influence of vacuum preloading, the induced inward lateral displacements are maximum at the surface and they gradually decrease with depth; larger lateral displacements lead to better compression and consolidation in soils (Cai *et al*. 2018). There is a decrease in the lateral displacement with depth which is because of the increase in shear strength of the soils along with depth in most of the cases (Ong and Chai 2011). Due to the application of vacuum, tension cracks are also formed on the ground up to a considerably large distance away from the vacuum consolidated area. For instance, a recent study from Bergado *et al*. (2021) reported ground cracks to be as far as 6 m from the edge to the sealing trench. The effects of these phenomena can be substantial in projects having structures adjacent to soil slopes (Robinson *et al*. 2012; Liu *et al*. 2018). Therefore, it becomes a crucial factor to be considered during the design as well as the operational phase.

In the present study, the site location was not well suited to soil improvement using surcharge due to its proximity to slopes and the consequent risk of soil failure. Vacuum consolidation in flat grounds is a common ground improvement procedure but research involving the use of vacuum consolidation near slopes has been rare and its effect on the slope movements has not been studied well. In this paper, the results from VCM were analysed, such as lateral movements, pore pressure, settlement and undrained shear strength. The changes in these parameters were monitored from the field data and the effect of vacuum pressure on the adjacent slope movements is presented. In addition, other factors were also investigated such as smear effects due to PVD installation, $C_h$ and the shear strength increase after the soil improvement (Bergado *et al*. 1991; Chu *et al*. 2004; Lam *et al*. 2015).

In summary, this paper presents the following: (i) the effect of VCM on mitigating the lateral movement and stability of slopes during and after the process; (ii) analysis of settlements and pore pressures from VCM; (iii) back analysis of $C_h$ and smear effect of settlement data; and (iv) before and after field investigation of soft soil properties such as undrained shear strength, water content, OCR and pre-consolidation pressures.

## 2. MATERIAL AND METHODS

### 2.1. Site location and condition

The housing project considered in the study was located in southern Bangkok, on King Kaew Road, Samut Prakan district near Suvarnabhumi Airport (Thailand), and the area has a soft-soil deposition ranging from 14–18 m depth below the ground level (Refer Figure 1). The site was located adjacent to a slope and consisted of two zones, namely: Zone 1 (3637 $m^2$) and Zone 2 (3482 $m^2$), as shown in Figure 2.

Boreholes BH-1 (Zone 1) and BH-3 (Zone 2), as well as Field Vane Tests FVT-1 (Zone 1) and FVT-4 (Zone 2), were performed before VCM. Similarly, boreholes BH-2 (Zone 1) and BH-4 (Zone 2), as well as Field Vane tests FVT-2 and FVT-3 in Zone 1 and FVT-5 and FVT-6 in Zone 2, were performed after VCM (Refer Figure 2). Some portion of Zone 2 initially had a shallow pond of about 1.5 m depth which was later filled by soft clay before the application of VCM.

Figures 3–5 show the site conditions during different stages of VCM in sequence starting from the PVD layout works to the operational stages. Figure 3 shows the site after the completion of sand blanket works and PVD installation. During the period of vacuum operation, the site was submerged with a water surcharge in both Zone 1 and 2 due to water discharge. The site along with the sealing trench adjacent to the slope is shown in Figure 4. From Figure 5 it can be observed that there was a formation of large tension cracks near the VCM zone because of inward lateral pull from the application of vacuum.

### 2.2. Borehole and soil properties

As shown in Table 1, the soil profile in Zone 1 was uniform with the topmost 3 m comprising a weathered clay layer with undrained shear strength values in the range of 20–30 kPa. These values were higher because of the upper layers being overconsolidated due to fluctuations in the groundwater level. Approximately 10 m of very soft to soft clay with low shear strength underlaid the weathered clay followed by a medium-stiff to stiff clay layer down to 18 m depth as shown in Figure 6. The natural water contents, Atterberg limits and soil type based on USCS Classification (ASTM 2017) are also indicated in Table 1. The groundwater table was located 1 m below ground level.

The soil profile and properties in Zone 2 are tabulated in Table 2. The topmost 1.5 m layer in Zone 2 consisted of soft clay fill. Underlying this was approximately 9 m of a

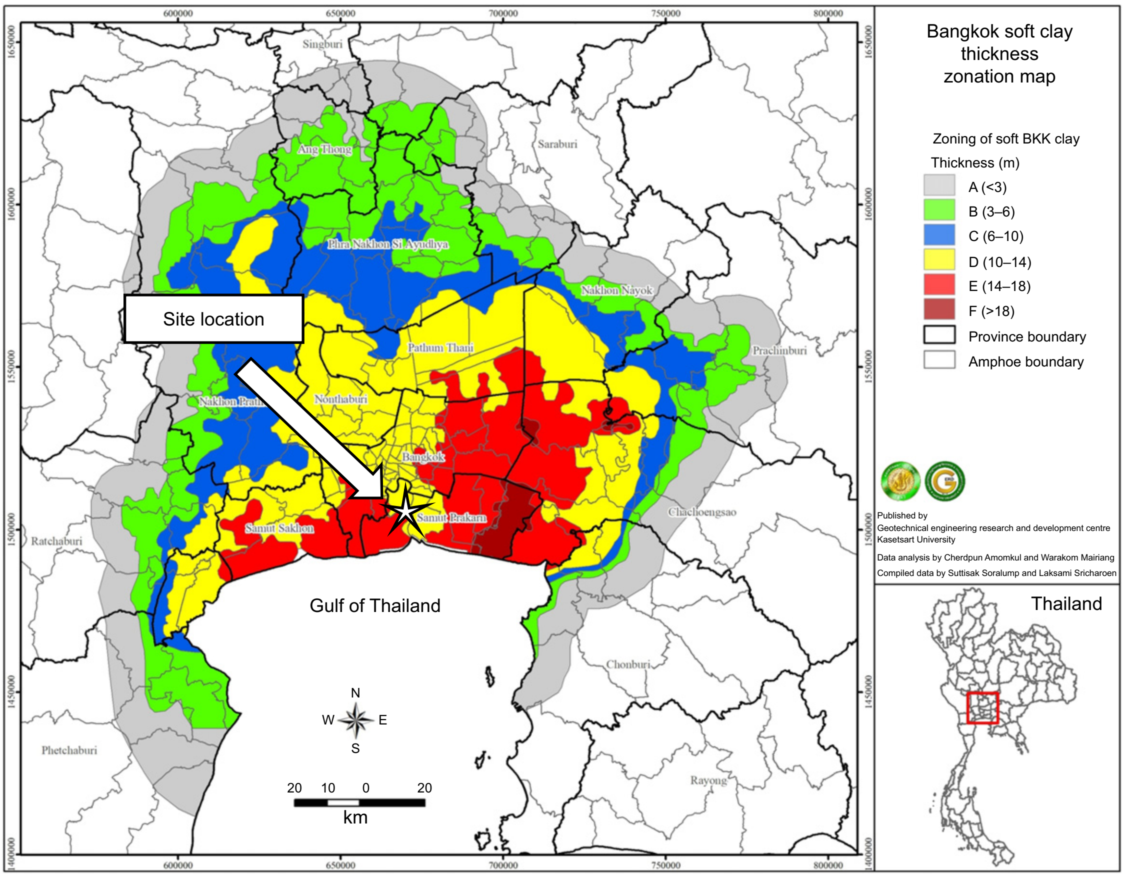


**Figure 1. Site location showing thickness and depth of soft Bangkok clay soft soil depth**

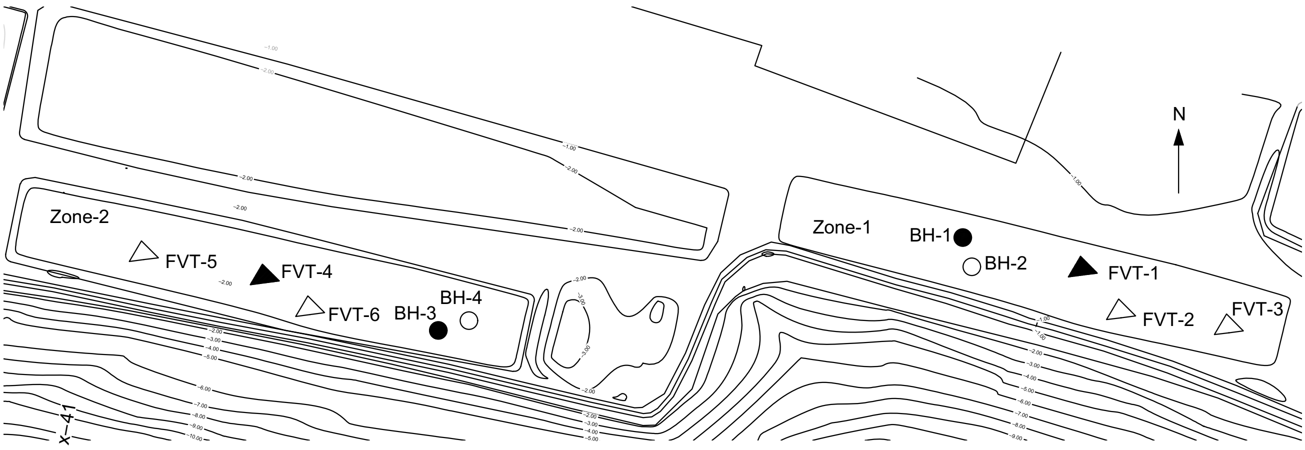


**Figure 2. Contours and field investigation layout of Zone 1 and Zone 2**

very soft to soft layer followed by a medium to stiff clay layer down to 18 m depth, as plotted in Figure 7. Similar to Zone 1, the natural water contents, Atterberg limits and soil type are also indicated in Table 2. As for Zone 2, the groundwater is located around 1.2 m depth.

### 2.3. Instrumentation and method

The VCM method used an air-tight sheet membrane installed on top of a 0.3 m sand blanket placed over the topsoil. PVDs with a length of 10 m were installed at a spacing of 0.8 m in a triangular pattern. The total width of the PVD installation was 18 m; a 1.5 m wide trench on both sides was used for sealing the area as shown in Figure 8. The detailed properties of PVDs are shown in Table 3.

Instruments were set up on site to monitor the parameters such as vacuum pressure, surface settlement, pore water pressure and lateral movements in the slope. The instruments were installed in a similar pattern and the same order in both zones. A plan and sectional view for Zone 2 are shown in Figures 8 and 9 respectively. The instrumentation of each zone consisted of three settlement

**Figure 3. PVD Layout and installation in site (Zone 1)**

**Figure 4. Slope area in Zone 2**


**Figure 5. Tension cracks near slope (Zone 1)**

plates and vacuum gauges each, 1 piezometer and 1 inclinometer. The vacuum pumps were kept submerged in a water-filled trench as they were water submersible and specifically used for vacuum preloading purposes. The discharge capacity was 45 $m^3$/h and they operated at a frequency of 50 Hz, rated voltage of 380 V and current of 15 Å. A pipe of diameter 65 mm was connected to the pump for creating a vacuum and the pump pressure was monitored using vacuum gauges throughout the preloading period. The average pressure during the vacuum consolidation was in the range of 75–85 kPa except during power outages.

The vacuum gauges used for monitoring the pump pressure were capable of measuring a maximum pressure of up to 100 kPa and were placed in the center of the embankment along with the settlement plates. The settlement plates were placed above the geomembrane and connected to a riser rod and the level on the riser rod was recorded to measure the settlements. The pore pressure measurements were made using a push-in vibrating-wire piezometer installed at a depth of 6 m below the existing ground level. The piezometers were made of stainless steel, had a body diameter of 27 mm and were capable of measuring pressure up to 350 kPa. For the lateral movement monitoring, vertical inclinometer casings were installed down to 20 m depth, and the top level of the casing was 0.5 m above the ground surface. An inclinometer probe made of stainless steel having a body diameter of 27 mm was inserted into the casing and measurements of displacements were made in a down-up sequence in the interval of every 0.5 m.

## 3. RESULTS AND DISCUSSIONS

### 3.1. Effect of VCM on lateral movement of the adjacent slope

Generally, in adjacent areas surrounding the VCM zone, inward lateral displacements were observed due to the suction effect of the vacuum near the boundary. The lateral movements in the slopes near the VCM zone were monitored based on the inclinometers in Zone 1 and Zone 2, as indicated in Figures 10a and 10b respectively. The measurements made before the start of pumping showed outward lateral movements in the slope in both the Zones 1 and 2 because of the surcharge load from vehicles and construction equipment.

In Zone 1 before the start of pumping on 30th January, there was around 24 mm outward movement during the interval of 2 weeks (see Figure 10a). Similarly, in the case of Zone 2, there was 20 mm movement, as indicated in Figure 10b. The slope movement was very substantial in the upper 5 m of the soil profile and the movements decreased with depth. The depth of very soft soil in Zone 1 was up to 13 m and the outward movements corresponded closely to the soft soil depth.

During the VCM, the outward movements in the slope substantially reduced and remained less than the initial values after the termination of vacuum pumping. Figure 11 indicates the rate of movement before, during and after VCM in Zone 1. Figure 11a shows the lateral movement before VCM. Figures 11b and 11c indicate that during VCM, the outward lateral movements in Zone 1 were reduced throughout the top 5 m of the soil profile. Similarly, in Zone 2, before the start of VCM on 23 July, the outward movement was nearly 8–10 mm/week in the top 4 m of the soil profile and during VCM, the outward

**Table 1. Soil properties in Zone 1 before improvement**

| BOREHOLE-1 | | | | | | OCR | Max. past pressure (kPa) | $C_v$ ($m^2$/yr) |
|---|---|---|---|---|---|---|---|---|
| Depth (m) | Soil type (USCS) | Avg. $S_u$ (kN/$m^2$) | Avg. $W_n$ (%) | LL | PL | | | |
| 0–1.5 | Top soil | 27.2 | 50 | 86.0 | 34.9 | | | |
| 1.5–3 | CH (Medium gray) | 24.1 | 55.2 | | | 1.25 | 50 | 2.26 |
| 3–13.5 | CH(Very soft-soft) | 11.7 | 102.0 | 113.2 | 43.9 | 1 | 63 | 0.41 |
| 13.5–18 | CH (Medium stiff-stiff) | 29.3 | 57.3 | | | 1.3 | 105 | 0.74 |

Note: Undrained shear strengths are as per standard testing procedures (ASTM 2013).
LL and PL are from samples at depths of 1.5 m and 9.25 m depth.
OCR, Max. past pressure and $C_v$ from samples at depths of 3.25 m, 9.25 m and 13.75 m.

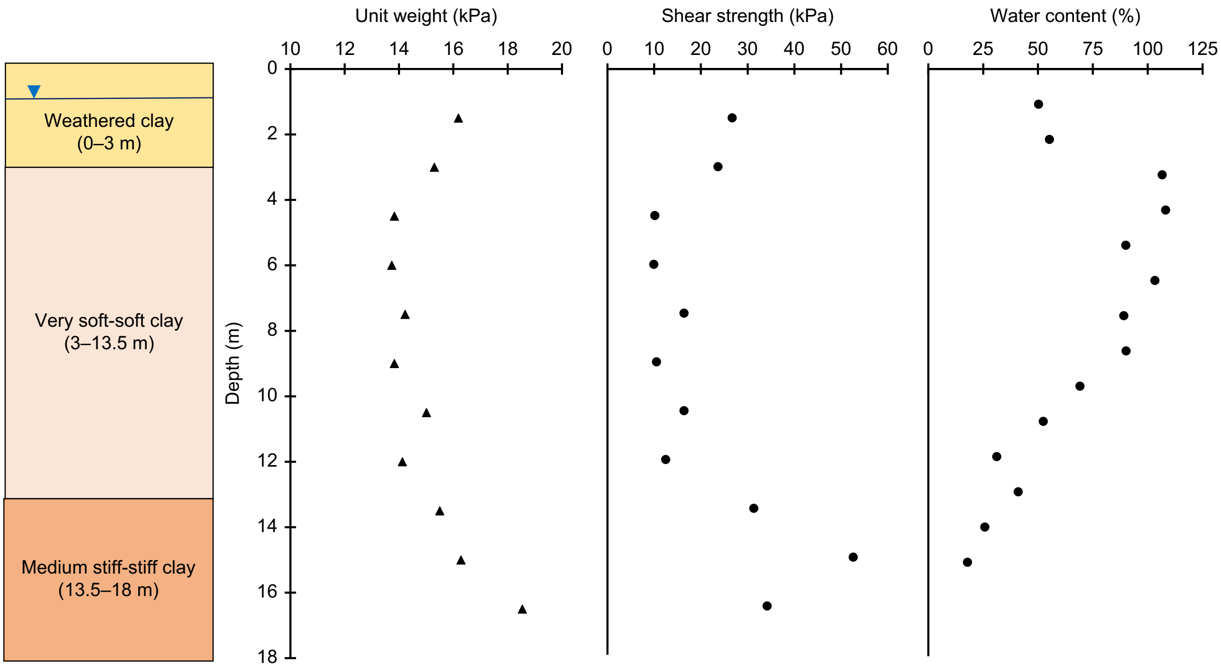


**Figure 6. Soil profile and properties in Zone 1**

**Table 2. Soil properties in Zone 2 before improvement**

| BOREHOLE-3 | | | | | | OCR | Max. past pressure (kPa) | $C_v$ ($m^2$/yr) |
|---|---|---|---|---|---|---|---|---|
| Depth (m) | Soil type (USCS) | Avg. $S_u$ (kN/$m^2$) | Avg. $W_n$ (%) | LL | PL | | | |
| 0–1.5 | Fill | 9.1 | 44 | 91.9 | 41.4 | 2.1 | 53 | 0.27 |
| 1.5–9 | CH (Very soft) | 9.5 | 115.2 | 145.5 | 49.7 | 1 | 37 | 1.14 |
| 9–10.5 | CH (Soft) | 15.7 | 84.5 | | | 1.3 | 68.67 | 0.73 |
| 10.5–16 | CH (Medium stiff) | 22.2 | 57.3 | | | | | |
| 16.5–18 | CH (Stiff-very stiff) | 51.9 | 32.0 | 54.0 | 20.3 | | | |

Note: Undrained shear strengths are as per standard testing procedures form (ASTM 2013).
LL and PL are from samples at depths of 1.5 m, 6.5 m, and 19.75 m.
OCR, Max. past pressure and $C_v$ from samples at depths of 1.75 m, 6.25 m and 9.25 m.

lateral movements decreased. Furthermore, the lateral movement was high during 5 to 14 September as shown in Figure 11b because of the loss of vacuum pressure in the Zone due to an electrical power interruption.

The reduced outward movement in both Zones 1 and 2 could have been due to the inward lateral pull toward the center of the preloading area caused by the effect of VCM (Chai *et al.* 2005; Liu *et al.* 2018). The inward displacement counteracted the outward movement in the slope and made the slope relatively stable during and after VCM, as shown in Figures 11b and 11c. The measurements of lateral movements after VCM were lower than the corresponding values before VCM as shown in Figures 11a and 11c. Comparison of the lateral movements after VCM in these two zones shows that Zone 1 still experienced outward movements while the corresponding

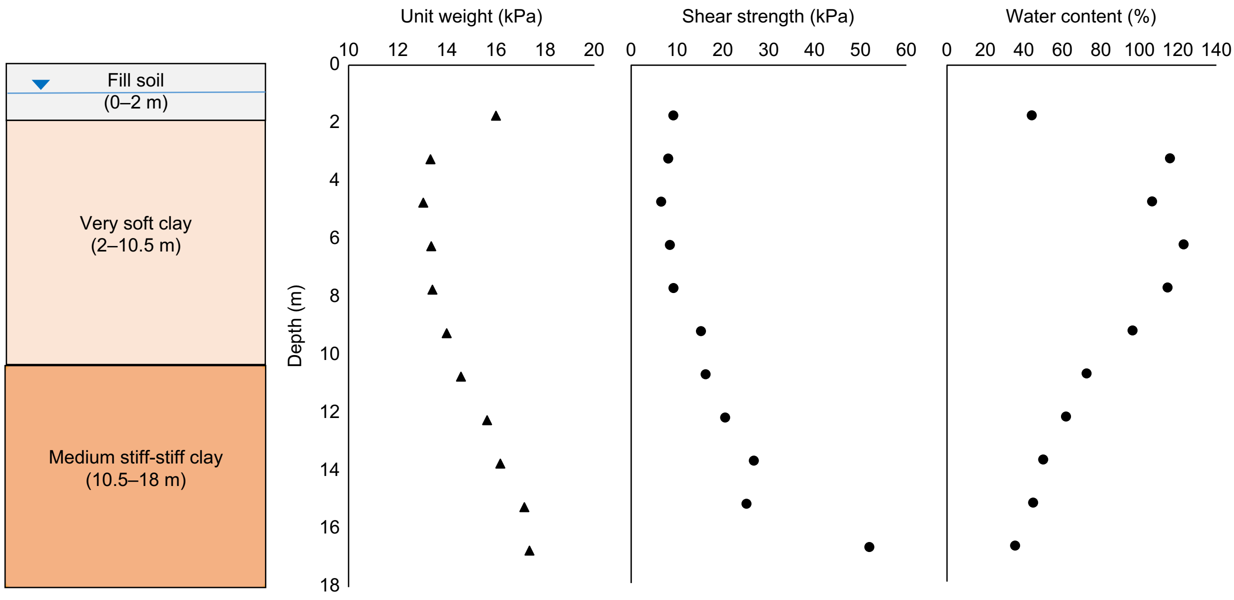


**Figure 7. Soil profile and properties in Zone 2**

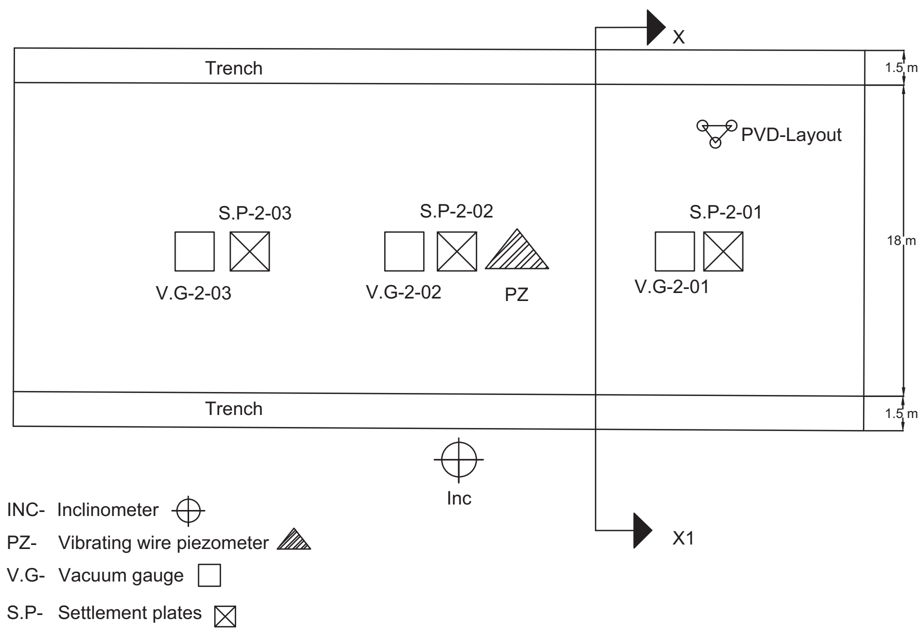


**Figure 8. Typical plan of VCM instrumentation**

**Table 3. PVD's parameters**

| PVD parameters | Unit | Value |
|---|---|---|
| Type | | Alidrain |
| Nominal width | mm | 100 |
| Nominal thickness | mm | 4.5 |
| Composite tensile strength (Full width test) | kN | 2.8 |
| Discharge capacity | $m^3/s$ | $150 \times 10^{-6}$ |
| Apparent opening size of filter | µm | 75 |
| Coefficient of permeability of filter | m/s | $1 \times 10^{-4}$ |
| Tensile strength of filter | kN/m | 7.5 |

lateral movements in Zone 2 were almost negligible as compared to the initial values. The initial high lateral movements in Zone 1 could have been due to the pore pressure rise and rebound effect in the adjacent VCM zone after the termination of vacuum pressure, as shown in Figure 12. The reductions in outward movement during and after the operation of VCM indicated that it can be a suitable method for soil improvement in adjacent areas and where slope stability issues are critical. However, the field monitoring data in this case only recorded the movement and stability of the slopes during and, for a short period after the soil improvement. The long-term movement and stability of slopes due to VCM needs to be investigated further.

### 3.2. Pore pressure behaviour during VCM

The pore pressures in both zones were monitored using vibrating wire piezometers installed at 6 m depth. The reduction in pore pressure with time corresponding to

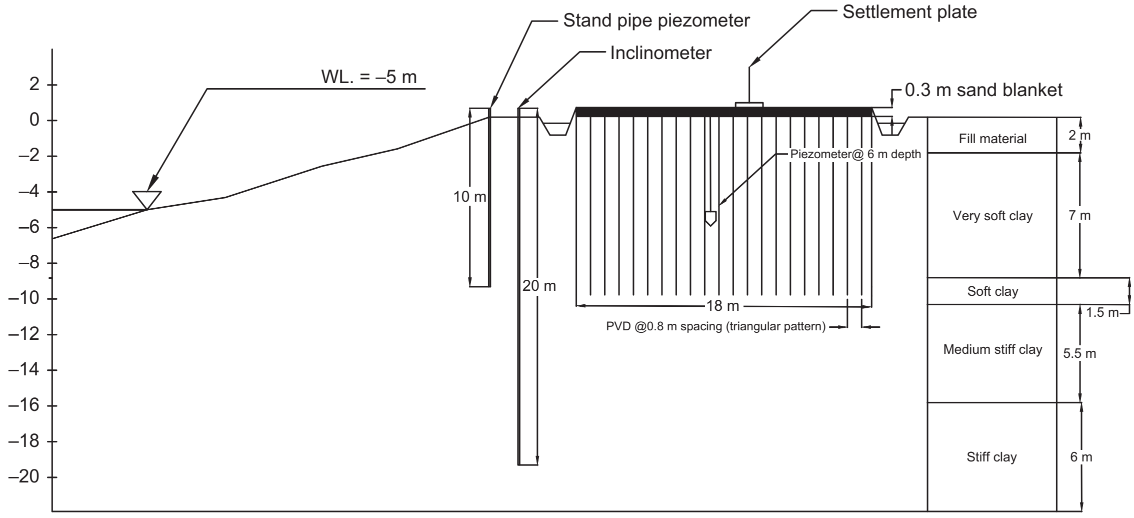


**Figure 9. Cross-section X-X1 with subsoil profile**

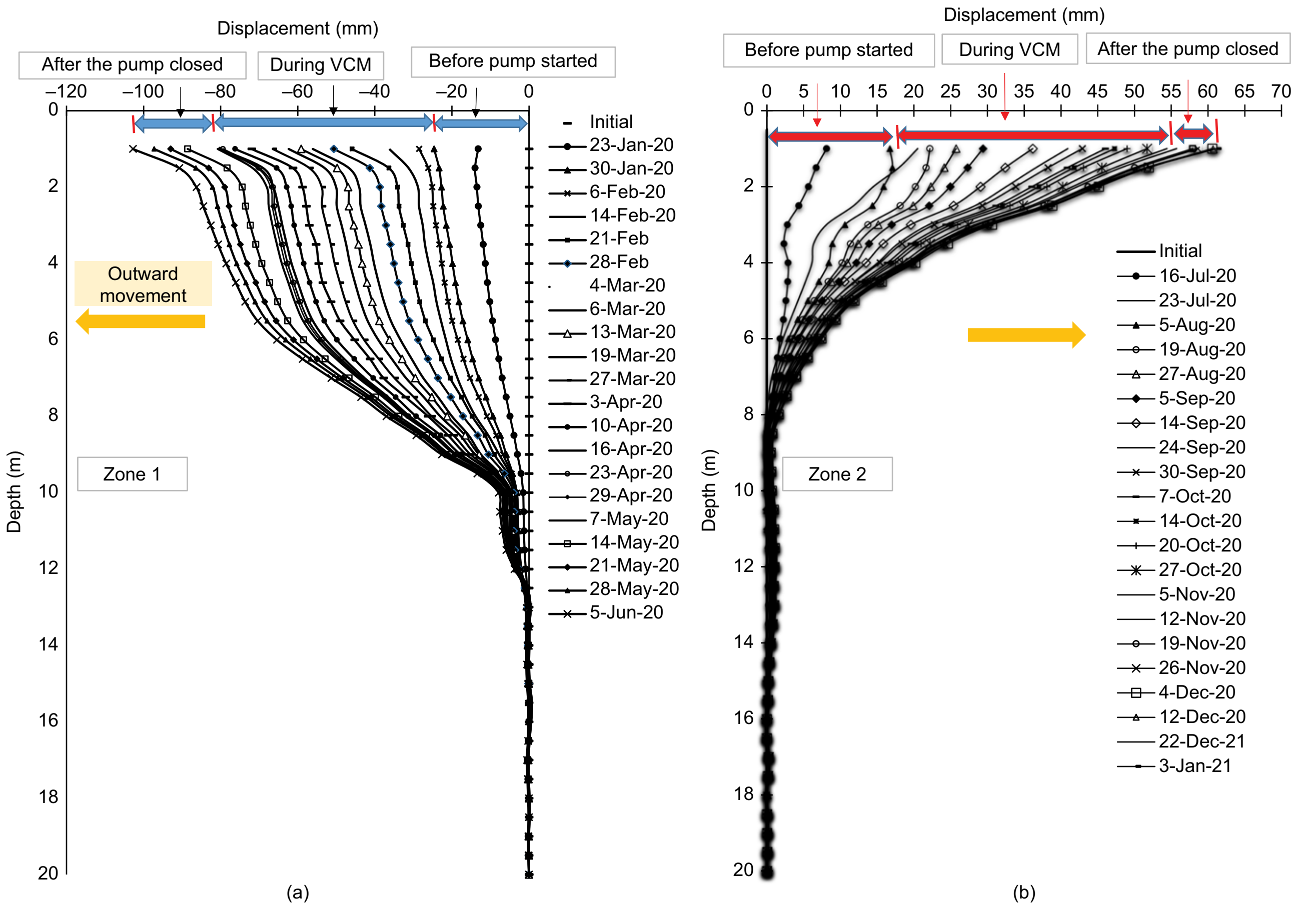


**Figure 10. Lateral movements from inclinometers (a) Zone 1; (b) Zone 2**

available vacuum pressure is plotted in Figure 12. In Zone 1, the initial pore pressure was 42 kPa which corresponded to the hydrostatic pressure considering the groundwater level is 1.2 m below the ground surface. Under constant vacuum pressure, the pore pressure gradually dissipated and showed no fluctuations until the end of the preloading period and the final value was –21 kPa. In vacuum preloading research, the difference in initial and final pore pressure is generally considered as available vacuum pressure (Qiu *et al.* 2007). Considering this, at the depth of 6 m, the available vacuum pressure was around 80% of the applied vacuum pressure.

In contrast, in Zone 2, the initial pore pressure measured at 6 m depth was 70 kPa (Figure 12) which was higher than the hydrostatic pressure, with excess pore pressure of about 22 kPa (G.W.L is at –1.2 m)

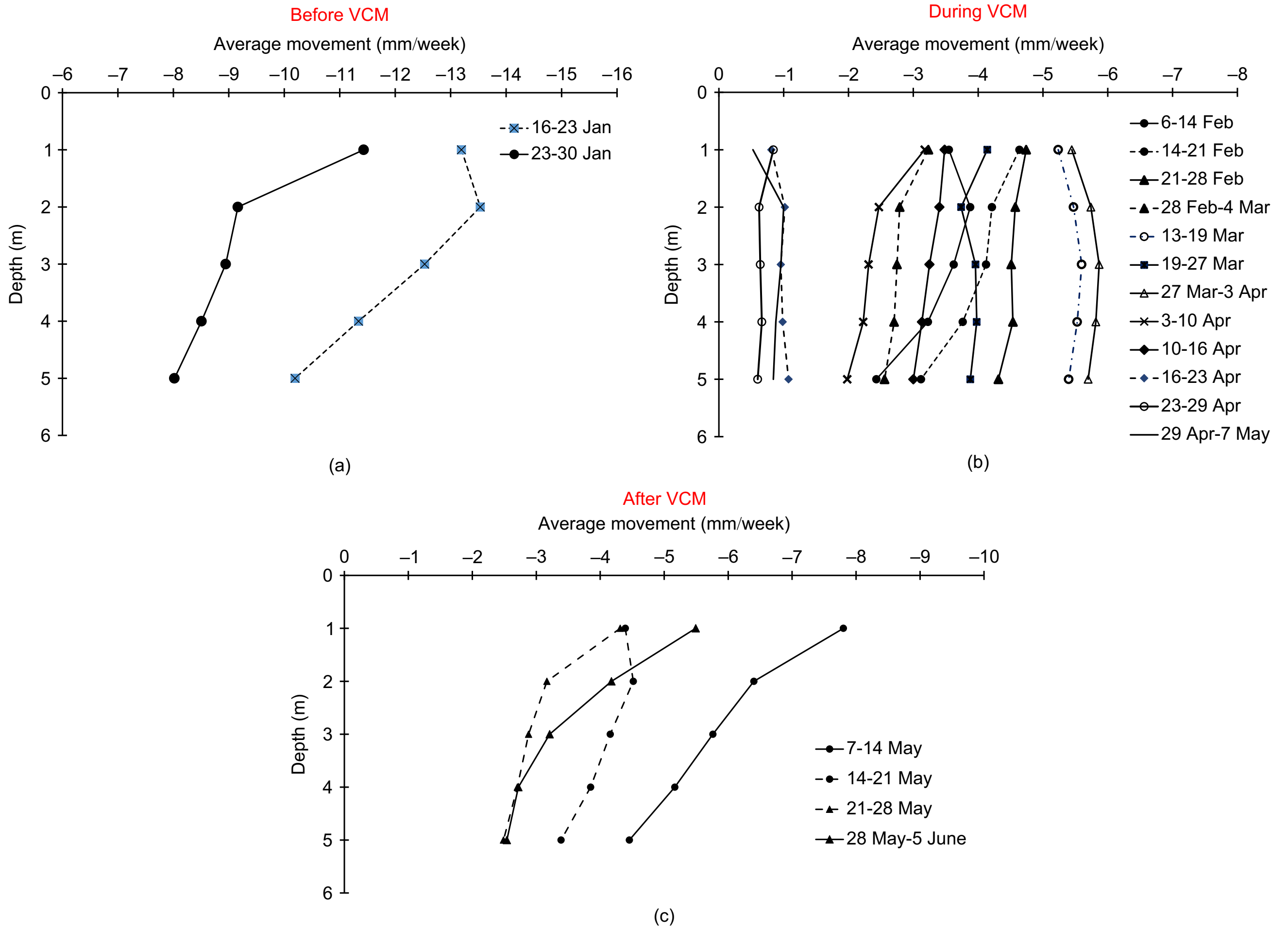


**Figure 11. Lateral movement with depth in Zone 1**

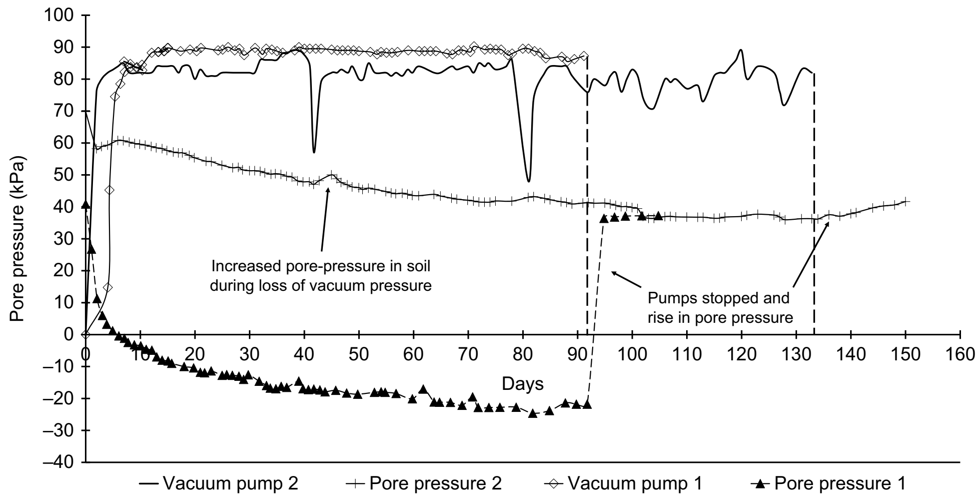


**Figure 12. Pore pressure variation with vacuum pressure**

because of the generation of excess pore pressure during installation and also due to the filling of topsoil. When there was a reduction in vacuum pressure on days 40 and 80 because of a power shortage, the pore pressure values fluctuated and then returned to a stable value once the pumps were operating normally again. After releasing the pump pressure, there was a gradual increase in pore pressure in Zone 2, as compared to a sudden rise in Zone 1. The difference in the trend of pore pressure reduction between Zones 1 and 2 during VCM and after the termination of vacuum pressure could be attributed to many different factors such as the in situ soil structure and the location of the piezometers with respect to the PVD.

In Figure 12, the pore pressures measured in Zone 2 were much lower than in Zone 1. However, the settlements measured in Zone 2 were similar to Zone 1 (refer to Figure 13). Zhang *et al*. (2021) reported that the pore pressure variation is not directly correlated to the settlement distribution but also the compressive characteristics of the soil in the surrounding area. However, besides this, it could also be because of a problem with the piezometer that was installed in Zone 2. In addition, field observations indicated that fluctuations in pore pressure reductions in the clay layer were related to the magnitude of vacuum pressure available during that time. Owing to this fact, where there was an absence of external surcharge loading to increase the pore pressure in the soil, the only change in pore pressure was due to vacuum pressure.

### 3.3. Field settlement during VCM

The surface settlements during the preloading period are shown in Figure 13. In both Zones 1 and 2, there was uniform settlement throughout the zone from preloading. The final settlement values recorded based on the settlement plates placed in different locations are plotted in Figure 13. The average rate of settlement per day was plotted for the time during VCM and 2 weeks post the VCM period. The settlement rates were the highest during the first 20 days by as much as 6 mm/day after the pump was turned on and gradually reduced with time (Figure 14). Around the end of preloading, the settlement rate had reduced to nearly 1 mm/day, indicating the end of vacuum preloading. The reduction in settlement rate towards the end of preloading can be explained by the increase in effective stress and a considerable amount of consolidation being achieved due to pore pressure dissipation. After the termination of vacuum pressures, rebounds in the improved ground were observed of up to 5 cm in 20 days as shown in Table 4. Table 4 presents the magnitude of final settlements from the field. A higher settlement was recorded in Zone 2 compared to Zone 1 because the soil in this area was relatively weaker with lower undrained shear strength and higher water content.

### 3.4. Estimation of the degree of consolidation (DOC) and back analysis of consolidation parameters

The final settlement under primary consolidation and the degree of consolidation (DOC) in the field were back-calculated using the observational method proposed by Asaoka (1978). The plots for final settlement based on this method for Zones 1 and 2 are plotted in Figures 15a and 15b, respectively. The final settlement under primary consolidation was also calculated based on the 1-D method and compared to the back-calculated values from Asaoka's method. The obtained final values are presented in Table 5. The values obtained from both methods were in good agreement and for both Zones 1 and 2, the DOC values were above 80%.

The horizontal coefficient of consolidation was then back-calculated using the final settlement obtained from Asaoka's method and the equation proposed by Hansbo (1979, 1981) for calculating radial consolidation by PVD improvements:

$$U_{\mathrm{h}} = 1 - \exp(-8T_{\mathrm{h}}/F) \tag{1}$$

$$F = F(n) + F_s + F_r \tag{2}$$

where

The values of $F(n)$, $F_{\mathrm{s}}$ and $F_{\mathrm{r}}$ are given by the following equations:

$$F(n) = \ln\left(\frac{D_{\mathrm{e}}}{d_{\mathrm{w}}}\right) - \frac{3}{4} \tag{3}$$

$$F_{\mathrm{s}} = \left(\frac{K_{\mathrm{h}}}{K_{\mathrm{S}}} - 1\right)\ln\left(\frac{d_{\mathrm{s}}}{d_{\mathrm{w}}}\right) \tag{4}$$

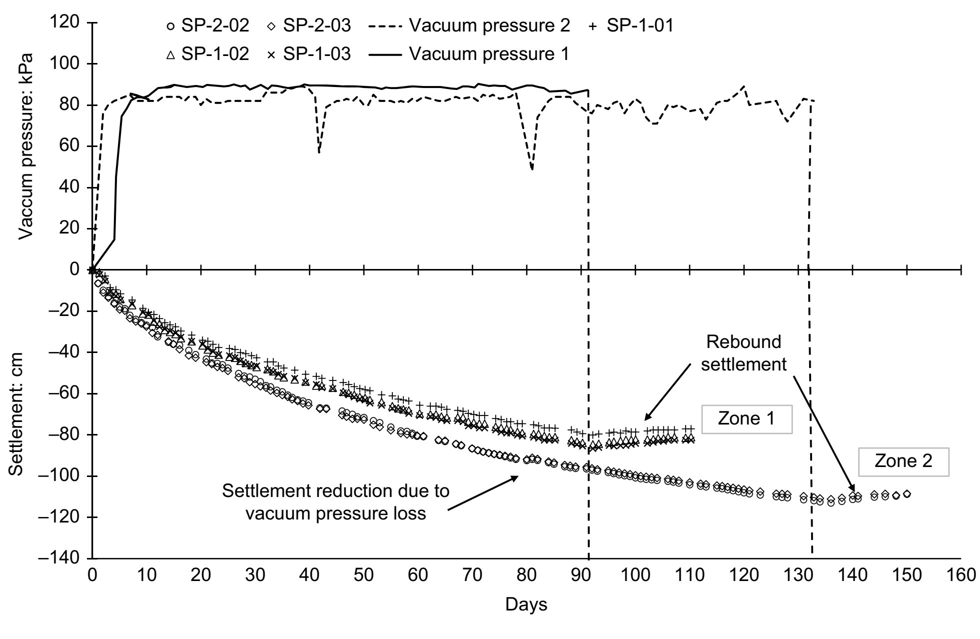


**Figure 13. Settlement comparison for different zones**

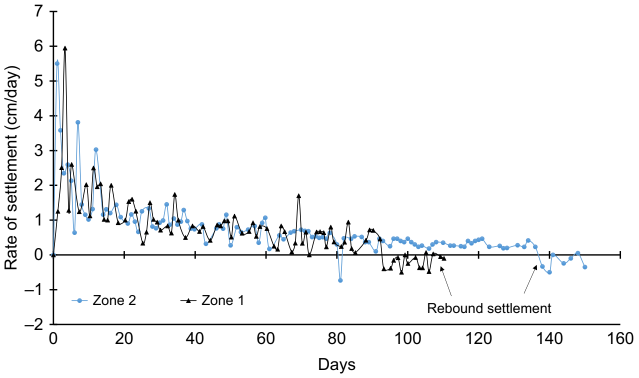


**Figure 14. Rate of settlement with time**

**Table 4. Observed field settlement**

| | Settlement (cm) | Rebound (cm) | Post rebound final settlement (cm) |
|---|---|---|---|
| SP-1-01 | 80.1 | 3 | 77.1 |
| SP-1-02 | 84.6 | 2 | 82.6 |
| SP-1-03 | 86.6 | 5 | 81.6 |
| SP-2-01 | 76.3 | 2.5 | 74.4 |
| SP-2-02 | 111.9 | 3.1 | 108.8 |
| SP-2-03 | 110.3 | 1.8 | 108.5 |

$$F_r = \frac{2}{3}\pi L^2 \frac{K_h}{q_w} \tag{5}$$

$$T_h = \frac{C_h t}{De^2} \tag{6}$$

$D_e = 1.05$* PVD spacing = 0.8 m (for triangular pattern) = 0.84 m, $d_m = 0.0925$ m

$$d_w = \frac{b+t}{2} = \frac{100+5}{2} = 0.052\,\text{m}$$

In practical use of PVD, the discharge capacity of drains is generally very high ($q_w > 50$ m$^3$/yr). Thus, the value of $k_h/q_w$ in Equation (5) becomes very small and the value of $F_r$ becomes negligible in calculating $F$ as well as the value of $C_h$.

In Zone 1, all the settlement plates had almost the same rate of settlement and final settlement value at the end of preloading. Thus, SP-1-01 was used for calculating final settlement and $C_h$. The final settlement for SP-1-01 was 97.43 cm (Figure 15) and based on this, the value of back-calculated $C_h$ was 2.7 m$^2$/yr for a corresponding $k_h/k_s$ value of 2. For SP-2-02 the ultimate settlement was calculated to be 126.3 cm and for a $k_h/k_s$ value of 2, $C_h$ was 2.43 m$^2$/yr. Figure 16 compares the predicted and observed settlements and can be seen to be in good agreement. Furthermore, the obtained values of $C_h$ from the site agreed with previous research for similar preloading cases. For example, Long *et al.* (2013) reported $C_h$ values from 2–4 m$^2$/yr and Saowapakpiboon *et al.* (2010a) obtained a $C_h$ value of 3.51 m$^2$/yr corresponding to $k_h/k_s$ values of 2 and 6.6 respectively, for the Suvarnabhumi International Airport Project. Long *et al.* (2013) further reported the values of $C_h$ in the range 1.9–6 m$^2$/yr for different $d_s/d_m$ and $R_s$ values and also stated that the obtained values of $C_h$ were directly proportional to both $d_s/d_m$ and $R_s$. Figures 17a and 17b provide the back-calculated values of $C_h$ following the method of Hansbo (1979, 1981), and in this case, the $C_h$ values were between 1.9–6 m$^2$/yr for $R_s$ values in the range 2–5.

However, for $k_h/k_s$, other research for similar vacuum-PVD schemes has shown that the values can differ in a wide range, For example, Voottipruex *et al.* (2014) obtained the values to be between 5–10 and Lam *et al.* (2015) back-calculated the value to be 7. For vacuum-PVD improvement, the $k_h/k_s$ value is reduced compared to conventional PVD improvement due to the increased $k_s$ values caused by vacuum preloading.

### 3.5. Field stress state conditions and shear strength increment analysis

The inclinometer readings showed that the slope was in an active condition and the isotropic vertical incremental stress due to vacuum application could be expected to reduce with depth which would affect the final effective stress and shear strength. FVT and borehole tests were carried out in both zones before and after vacuum preloading. The initial effective overburden stress at a

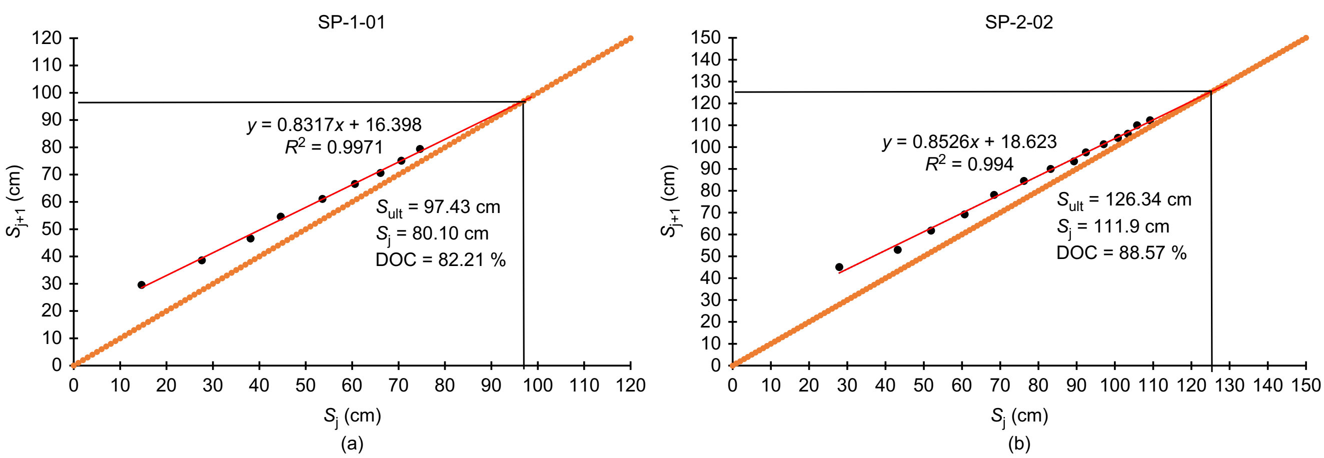


**Figure 15. (a) Asaoka plot for SP-1-01 to obtain ultimate settlement; (b) Asaoka plot for SP-2-02 to obtain ultimate settlement**

**Table 5. Final settlement and DOC values**

| | Zone 1 | | Zone 2 | |
|---|---|---|---|---|
| | Asaoka ($\Delta t = 7$) | 1-D Consolidation | Asaoka ($\Delta t = 7$) | 1-D Consolidation |
| $S_j$ (cm) | 80.1 | 84.6 | 111.9 | 111.9 |
| $S_{\mathrm{ult}}$ (cm) | 97.4 | 114.3 | 126.3 | 130.9 |
| DOC (%) | 82.1 | 70 | 88.6 | 85.4 |

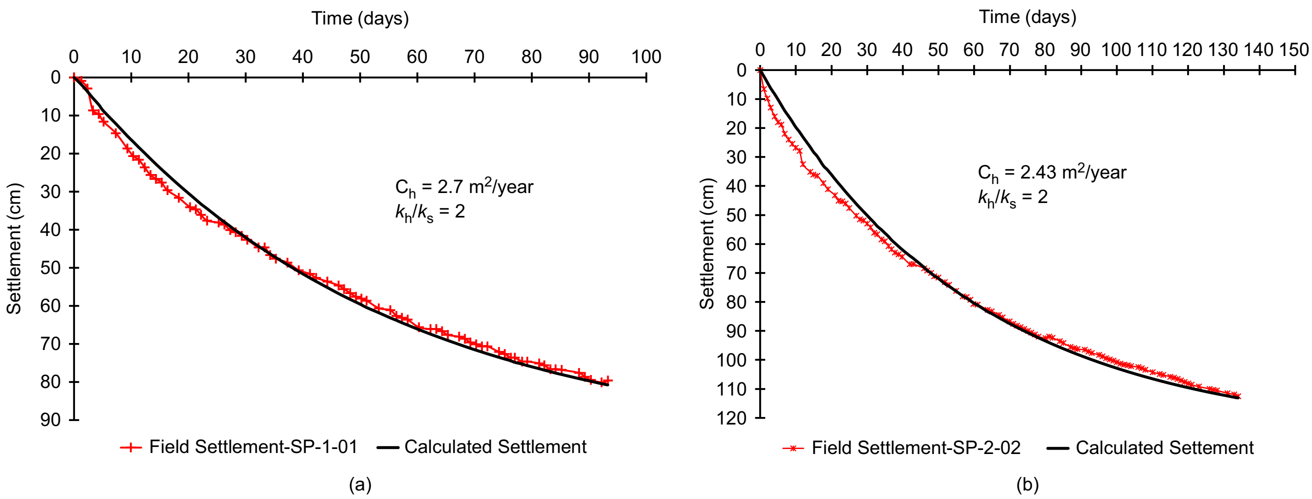


**Figure 16. (a) Comparison of predicted and observed field settlements for Zone 1; (b) comparison of predicted and observed field settlements for Zone 2**

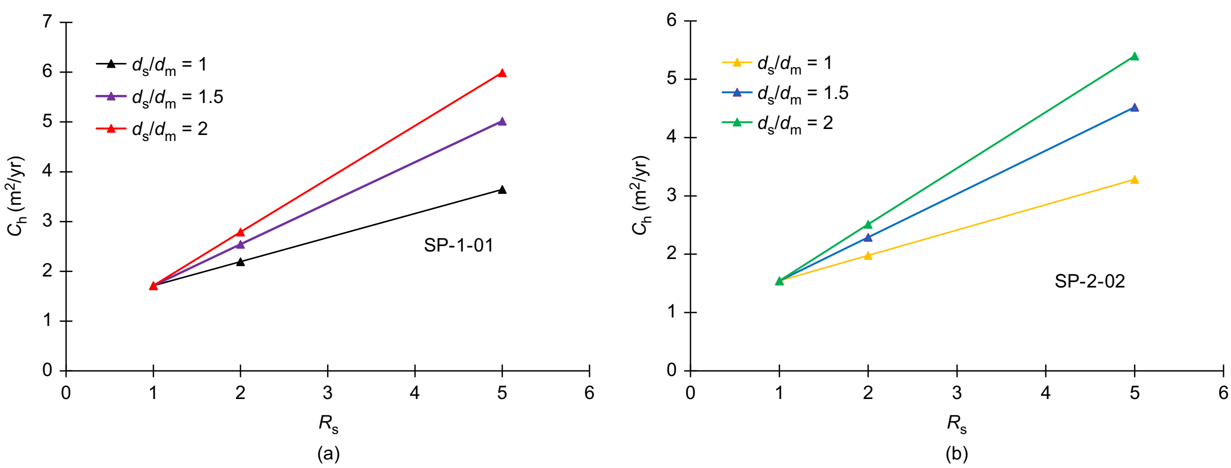


**Figure 17. (a) Back calculated values of $C_h$ for $R_s = k_h/k_s$ from SP-1-01; (b) back calculated values of $C_h$ for $R_s = k_h/k_s$ from SP-2-02**

depth of 6 m was around 37 kPa, if the additional stress due to vacuum was assumed to be 80 kPa, then the expected final undrained shear strengths using total stress and effective stress envelopes from the CU were 28 kPa and 40 kPa, respectively. The corrected final shear strength from FVT showed improvements but at a depth of 6 to 10 m, they were lower than the expected value of 25 kPa. It was suspected that the shear increments were not high because of the outward movement in the slope as the induced vertical stress is reduced in the active case and the soil might not gain the desired strength.

To check the validity of the assumption, the final shear strengths were calculated based on the following equation and then compared to the final values from FVT in the field (soil was in a, NC within the improvement depth):

$$T_f = T_o + U_Z \Delta\sigma_z \tan\varnothing_{cu} \quad (7)$$

The initial undrained shear strength values were obtained from field vane shear tests, the final DOC values were calculated from Asaoka (80% for Zone-1 and 90% for Zone-2), the total friction angle was taken from

CU-testing (10–15°) and the vertical stress due to vacuum loading on the equation was varied from 80 kPa at the top to 50 kPa at 10 m depth at the bottom of the PVD. The predicted final undrained shear strengths based on adopted values are presented in Figures 18a and 18b. The calculated shear strengths using Equation (7) matched well with the values from FVT after improvement.

From Figures 18a and 18b, it can be observed that the average shear strength increments in the upper soil profile were higher. Below the PVD (10 m depth), the improvement in shear strength was lowest in both zones, as expected.

The shear strengths increased by a maximum of 14 kN/m$^2$ at a depth of 7 m in Zone 1 as well as in Zone 2. Some discrepancies in values of observed final shear strength from FVT were observed in depths above 6 m in Zone 1 and in depths below 7 m in Zone 2, which could have been due to variation in the soil properties resulting from differences in the FVT locations.

The final undrained shear strength was also predicted using the initial values from UC-testing using Mesri's equation. Even though undrained shear strengths from UC-testing were comparatively lower than for the FVT tests, this method has been applied in several case histories and was applied in this case for soft-Bangkok clay, with the results compared to those from the conclusions of past research.

According to Mesri and Khan (2011), the increase in undrained shear strength can be expressed as:

$$\Delta S_{\mathrm{u}}(UC) = \frac{S_{\mathrm{uo}}}{\sigma'_p}\left[\left(P_{\mathrm{v}} - \sigma'_{\mathrm{p}} + \sigma'_{\mathrm{vo}}\right)\right] \quad (8)$$

Equation (8) shows that in the case of vacuum preloading without any surcharge, the increment in shear strength depends on available vacuum pressure, pre-consolidation pressure, and initial effective undrained shear strength. For the present case, the incremental vertical stress $\Delta\sigma_{\mathrm{v}}$ due to vacuum loading corresponds to the value $P_{\mathrm{v}}$ which was varied during the final shear strength prediction. For predicting the final shear strength, the value of vacuum pressure in the soils was varied similarly as in the case of FVT from 100% at the ground surface (80 kPa) to 60% (50 kPa) at a depth of 10 m. The predicted results with the use of the above-mentioned assumptions matched well with the field results. The UC test results of undisturbed soil samples from Zone 2 showed that the shear strengths increased by 1.5–4 times the initial undrained shear strengths but were below 30 kPa for most depths because of the increase in overburden stresses with depth. At a depth of 4.5–5 m and 6–6.5 m, the soil strength increased by approximately 17 kN/m$^2$ and 22 kN/m$^2$ respectively. This increase of 22 kN/m$^2$ shows an increment of 260% in the initial undrained shear strength. In the lower depths, – that is 9–9.5 m and 12–12.5 m, the shear strengths increased by approximately 9 kN/m$^2$ which is around a 40–60% increment in the initial undrained shear strengths at those depths (Figure 19a). The increase in shear strength from both the FVT and UC testing showed higher values

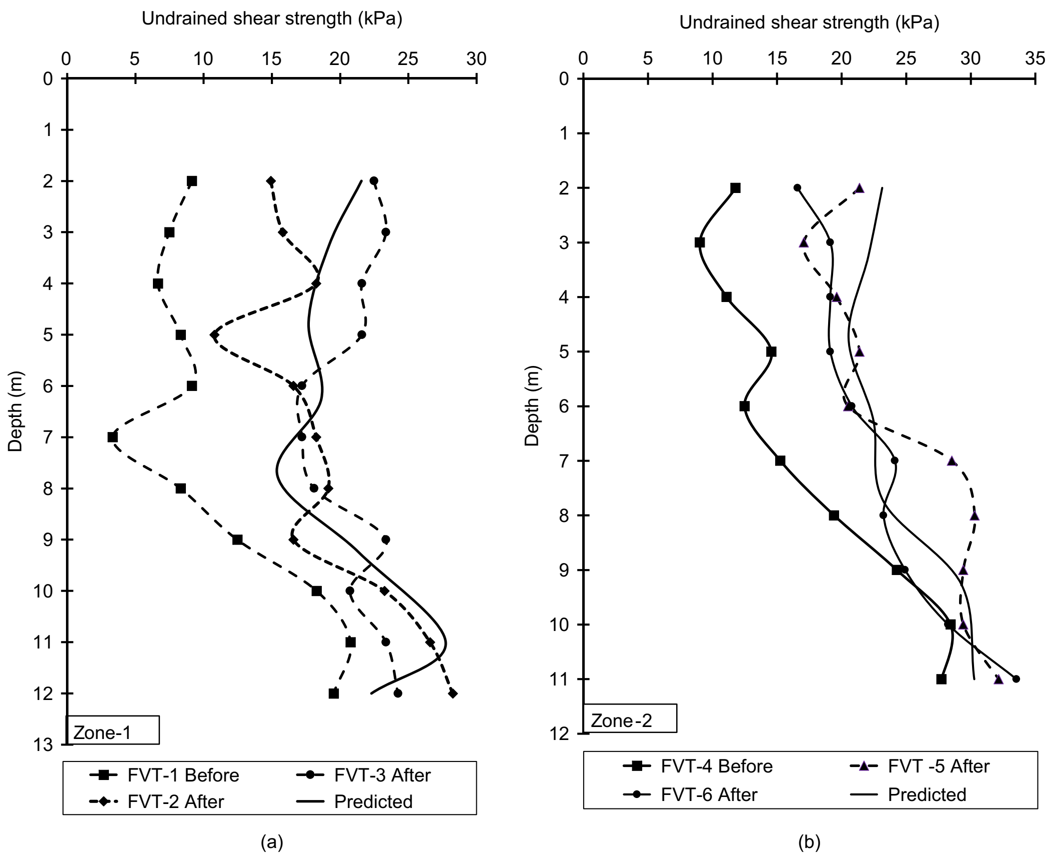


**Figure 18. (a) FVT results before and after VCM in Zone-1; (b) FVT results before and after VCM in Zone 1**

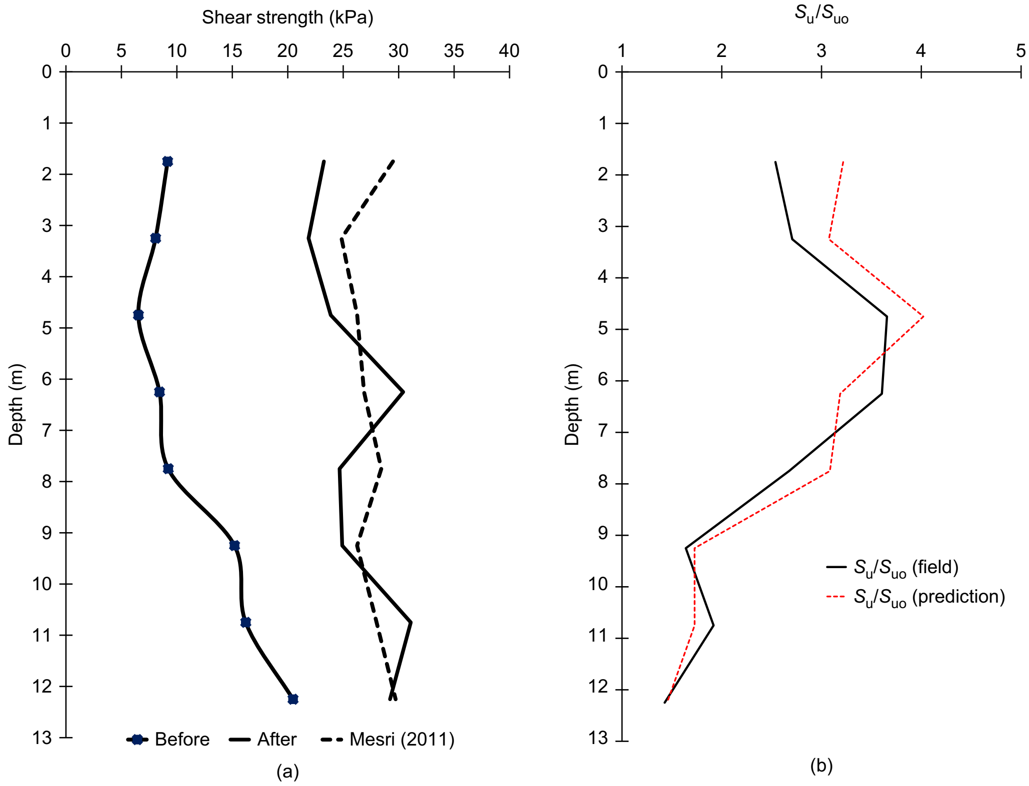


**Figure 19. (a) Measured and predicted shear strengths from UC-test in Zone 2; (b) $S_u/S_{uo}$ comparison from field and prediction**

in top regions and lower values at the bottom of the PVD which implied that there was more effective vacuum pressure in the upper soil profile and this reduced with depth. In addition, the shear strength values from FVT were already high in the lower regions, thus the strength values before and after improvement were not much different (Figures 19a and 19b).

For soft clays in which $S_{uo}$ or $\sigma'_{vo}$ increases with depth, $S_u/S_{uo}$ is expected to reduce and vice versa (Mesri and Khan 2011). Figure 19b illustrates a similar trend for a profile of $S_u/S_{uo}$ obtained in the field and for the predicted values. Up to a depth of 4.75 m, $S_u/S_{uo}$ increased as there was a decrease in the initial undrained shear strength with depth. With the increase in $S_{uo}$ from 4.75 m, the $S_u/S_{uo}$ values for both the field and predicted values decreased with depth.

### 3.6. Improvement in water content, over-consolidation ratio and maximum past pressure.

Improvement in the water contents, OCR and pre-consolidation pressures before and after vacuum consolidation are presented in Figure 20, showing that there was a considerable decrease in the water contents after VCM at most depths. However, the initial water content in Zone 1 was lower than the final value, which could have been due to the soil consisting of backfilled material. The initial water contents in both zones were very high, even higher than 100% for some depths. The reductions in water content mostly fluctuated with depth and were the largest mostly for mid-depths (4–9 m), as shown in Figure 20a. For lower depths (10–12 m) the reductions were low because there was no PVD. Overall, the water content reduction was in the range of 6–50% in the PVD improved zone. Consolidation tests were carried out in Zone 2 before and after VCM for samples at different depths (1.5–2 m, 6–6.5 m and 9–9.5 m). Figures 20b and 20c indicate that the maximum past pressure and OCR values increased with depth. Figure 20b shows that the top fill material was in an over-consolidated state and below that depth, the soil was in a normally to slightly over-consolidated state down to 10 m depth. In the upper zone, OCR increased from 2.08 to 2.5 after improvement. Also, initially, at 6–6.5 m depth and 9–9.5 m, the soil samples were in a normally consolidated to slightly over-consolidated state with an OCR of 1 and 1.28, respectively; and after improvement, the OCR values increased to 1.56 and 1.77, respectively.

At a depth of 6–6.5 m below the ground level, considering the depth of the groundwater table to be 1.2 m below the ground surface, the effective overburden stress was 37 kPa. In the absence of an external surcharge, the final effective stress at the end of primary consolidation in vacuum preloading can be written as:

$$\sigma'_{vf} = \sigma'_{vo} + P_{vac}$$

The additional load due to vacuum was 80 kPa, so the final effective stress from the given equation will be 107 kPa. The average DOC obtained from the surface settlement plates placed in Zone 2 was in an average of 87% (refer to Table 4). With an achieved DOC of 87%, the final maximum past pressure should be around 90 kPa but the maximum past pressure obtained at this depth was 75 kPa. This implies that the effective vacuum pressure at that depth was considerably less. It can be further observed that the

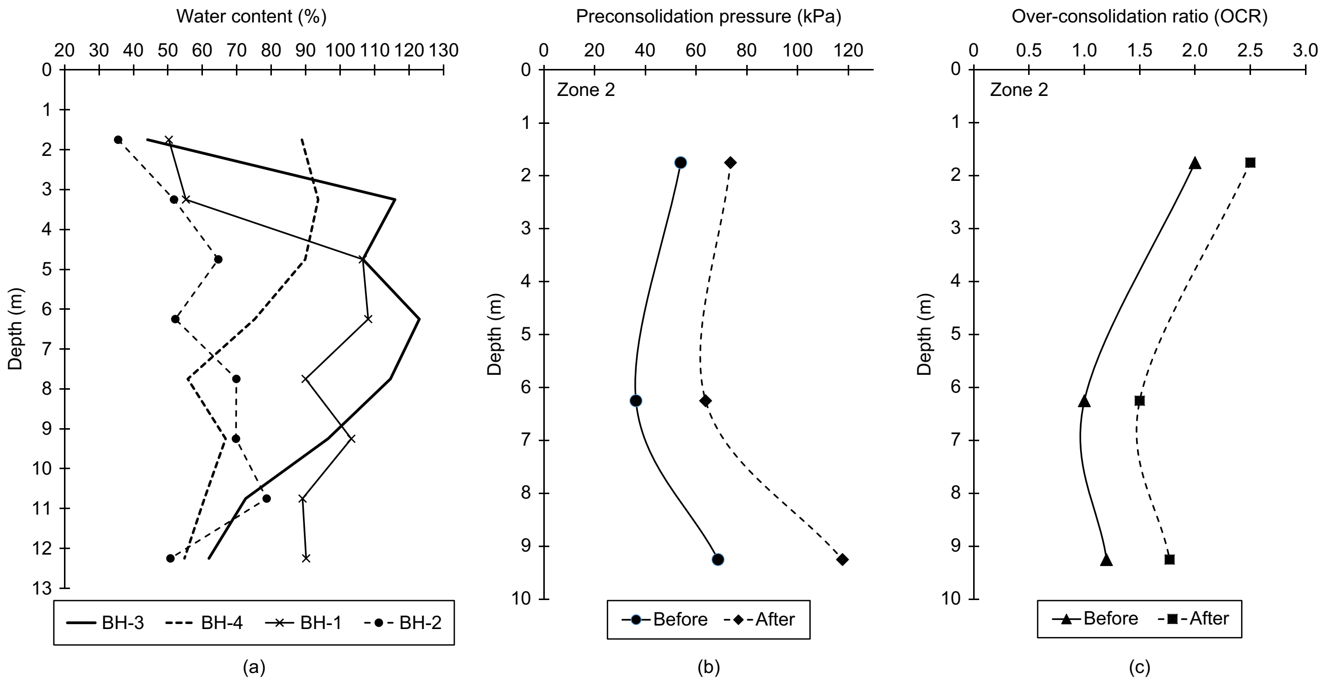


**Figure 20. Soil properties before and after improvement: (a) water content in Zone 1 and Zone 2; (b) preconsolidation pressure before and after improvement in Zone 2; (c) over consolidation ratio in Zone 2**

total pore pressure dissipation in Zone 2 was 37 kPa, which as mentioned earlier is considered as the available vacuum pressure during preloading, which further explains the maximum past pressure obtained. In addition, the predicted undrained strength based on reduced values of vacuum stress with the increase in depth also made a good agreement with field measurements.

## 4. CONCLUSIONS AND RECOMMENDATIONS

A soft clay site nearby a slope undergoing large lateral outward movements was successfully improved using the vacuum consolidation method, showing that VCM can be efficiently applied near critical slopes. The field monitoring data showed a reduction in movement rates in the slope during and after the soil improvement, qualitatively indicating the stabilization of slope and reduction in risk of slope failure. Post improvement field investigation results indicated reduction in water contents up to 50% throughout the PVD improvement depth, the undrained shear strengths showed increments up to 260% along with an increase in OCR and maximum past pressures indicating the efficacy of VCM use in improving soft soil.

From the analysis of field data, it was found that a DOC up to 90% was achieved in the field, the back analysis showed smear zones (zone of disturbance) around the drains to be twice the mandrel diameter for soft Bangkok clay and the corresponding $C_h$ values based on this were in between 2–3 $m^2$/yr, which are in good agreement with the values from past literature.

The experience from the field showed that difficulties might be encountered in reaching the desired maximum past pressure because of a reduction in vacuum induced overburden stress with depth. In addition to this, the observed behaviour in slope is not representative of long-term stabilization of slope but only the mitigation of lateral movements during and for some time after the soil improvement process. In soft soils, because their shrinkage and swelling properties dominate the short-term behaviour these are the critical aspects to be monitored and the results showed that after VCM completion they had no immediate significant impact on slope movement. However, the study of the long-term behaviour of slopes under similar scenarios is recommended to further strengthen the efficacy of VCM use near slopes.

## ACKNOWLEDGEMENTS

The Geotechnical Engineering Research and Development Center (GERD) and SILA Geotechnique. Co. Ltd provided help and support during the stages of the research. Professor Dennes T. Bergado contributed valuable comments during the stages of manuscript preparation.

## NOTATION

Basic SI units are shown in parentheses.

| | |
|---|---|
| $C_h$ | horizontal coefficient of consolidation ($m^2$/s) |
| $C_v$ | coefficient of vertical consolidation ($m^2$/s) |
| $D_e$ | equivalent diameter of the soil cylinder (m) |
| $d_m$ | diameter of the mandrel based on width and thickness (m) |
| DOC | degree of consolidation (dimensionless) |
| $d_s$ | smear zone diameter ($d_s = 2d_m$) (m) |

$d_w$ equivalent diameter of the prefabricated vertical drain (PVD) based on thickness and width (m)
$k_h$ horizontal permeability in the undisturbed zone (m/s)
$k_s$ horizontal permeability in the smear zone (m/s)
L drainage length (equal to the length of PVD for a single drainage) (m)
LL liquid limit (dimensionless)
OCR over-consolidation ratio (dimensionless)
PL plastic limit (dimensionless)
$q_w$ discharge capacity of drains ($m^3/s$)
$S_u$ final undrained shear strength after primary consolidation ($N/m^2$)
$S_{uo}$ initial undrained shear strength ($N/m^2$)
$T_f$ final undrained shear strength ($N/m^2$)
$T_h$ time factor for horizontal drainage (dimensionless)
$T_o$ initial undrained shear strength ($N/m^2$)
$t$ time (s)
$U_h$ degree of consolidation (DOC) for horizontal drainage expressed in percentage (dimensionless)
$U_z$ degree of consolidation (DOC) at the end of preloading expressed in percentage (dimensionless)
$W_n$ water content of the soil expressed in percentage (dimensionless)
$\Delta\sigma_z$ additional change in stress due to vacuum loading ($N/m^2$)
$\varnothing_{cu}$ undrained internal friction angle from the CU test (degrees)
$\sigma'_p$ pre-consolidation stress ($N/m^2$)
$\sigma'_{vo}$ initial overburden stress ($N/m^2$)

## ABBREVIATIONS

CU consolidated undrained test
FVT field vane shear test
G.W.L groundwater level
NC normally consolidated state in soils
PVD prefabricated vertical drain
UC unconfined compression test
VCM vacuum consolidation method

## REFERENCES

Abuel-Naga, H., Bergado, D. T. & Gniel, J. (2015). Design chart for PVD improved ground. *Geotextiles and Geomembranes*, **43**, No. 6, 537–546.

Alditra, D. F., Chaiprakaikeow, S. & Soralump, S. (2020). Study of VCM improved soft soil properties using non-destructive and destructive techniques. *Geosciences*, **10**, No. 8, 300.

Anda, R., Fu, H. T., Wang, J., Lei, H., Hu, X., Ye, Q., Cai, Y. & Xie, Z. (2020). Effects of pressuring timing on air booster vacuum consolidation of dredged slurry. *Geotextiles and Geomembranes*, **48**, No. 4, 491–503.

Asaoka, A. (1978). Observational procedure of settlement prediction. *Soils and Foundations*, **18**, No. 4, 87–101.

ASTM. D.2166/D2166M: *Standard test method for unconfined compressive strength of cohesive soil*. ASTM International, West Conshohocken, PA, USA.

ASTM. D.2487: *Standard practice for classification of soils for engineering purposes (Unified Soil Classification System)*. American Society for Testing Materials, West Conshohocken, PA, USA.

Bergado, D. T., Asakami, H., Alfaro, M. C. & Balasubramaniam, A. (1991). Smear effects of vertical drains on soft Bangkok clay. *Journal of Geotechnical Engineering*, **117**, No. 10, 1509–1530.

Bergado, D. T., Long, P. V. & Balasubramaniam, A. (1996). Compressibility and flow parameters from PVD improved soft Bangkok clay. *Geotechnical Engineering*, **27**, 1–20.

Bergado, D. T., Chai, J. C., Miura, N. & Balasubramaniam, A. S. (1998). PVD Improvement of soft Bangkok clay with combined vacuum and reduced sand embankment preloading. *Geotechnical Engineering*, **29**, No. 1, 95–122.

Bergado, D. T., Balasubramaniam, A. S., Fannin, R. J. & Holtz, R. D. (2002). Prefabricated vertical drains (PVDs) in soft Bangkok clay: a case study of the new Bangkok International Airport project. *Canadian Geotechnical Journal*, **39**, No. 2, 304–315, https://doi.org/10.1139/t01-100.

Bergado, D. T., Chaiyaput, S., Artidteang, S. & Nguyen, N. T. (2020). Microstructures within and outside the smear zones for soft clay improvement using PVD only, Vacuum-PVD, Thermo-PVD and Thermo-Vacuum-PVD. *Geotextiles and Geomembranes*, **48**, No. 6, 828–843.

Bergado, D. T., Jamsawang, P., Kovittayanon, N., Baez, F. & De Zwart, P. T. (2021). Vacuum-PVD improvement: a case study of the second improvement of soft Bangkok clay on the subsiding ground. *International Journal of Geosynthetics and Ground Engineering*, **7**, No. 4, 1–20.

Bergado, D. T., Jamsawang, P., Jongpradist, P., Likitlersuang, S., Panteng, C., Kovittayanun, N. & Baez, F. (2022). Case study and numerical simulation of PVD improved soft Bangkok clay with surcharge and vacuum preloading using modified air-water separation system. *Geotextiles and Geomembranes*, **50**, No. 1, 137–153.

Cai, Y. Q., Xie, Z. W., Wang, J., Wang, P. & Geng, X. Y. (2018). New approach of vacuum preloading with booster PVDs to improve deep marine strata. *Canadian Geotechnical Journal*, **55**, No. 10, 1359–1371.

Chai, J. C., Carter, J. P. & Hayashi, S. (2005). Ground deformation induced by vacuum consolidation. *Journal of Geotechnical and Geoenvironmental Engineering*, **131**, No. 12, 1552–1561.

Chai, J. C., Carter, J. P. & Hayashi, S. (2006). Vacuum consolidation and its combination with embankment loading. *Canadian Geotechnical Journal*, **43**, No. 10, 985–996.

Chai, J. C., Miura, N. & Bergado, D. T. (2008). Preloading clayey deposit by vacuum pressure with cap-drain: analyses versus performance. *Geotextiles and Geomembranes*, **26**, No. 3, 220–230.

Chai, J. C., Ong, C. Y., Carter, J. P. & Bergado, D. T. (2013). Lateral displacement under combined vacuum pressure and embankment loading. *Geotechnique*, **63**, No. 10, 842–856.

Chai, J. C., Fu, H. T., Wang, J. & Shen, S. L. (2020). Behavior of a PVD unit cell under vacuum pressure and a new method for consolidation analysis. *Computer and Geotechnics*, **120**, 103415, https://doi.org/10.1016/j.compgeo.2019.103415.

Chai, J. C., Lu, Y. & Fu, H. (2021). Groundwater level under vacuum consolidation. *Proceedings of the Institution of Civil Engineers - Ground Improvement*, **174**, No. 2, 79–84.

Choa, V., Bo, M. W. & Chu, J. (2001). Soil improvement works for changi east reclamation project. *Proceedings of the Institution of Civil Engineers-Ground Improvement*, **5**, No. 4, 141–153.

Chu, J., Yan, S. W. & Yang, H. (2000). Soil improvement by the vacuum preloading method for an oil storage station. *Geotechnique*, **50**, No. 6, 625–632.

Chu, J., Bo, M. W. & Choa, V. (2004). Practical considerations for using vertical drains in soil improvement projects. *Geotextiles and Geomembranes*, **22**, No. 1–2, 101–117.

Chu, J., Bo, M. W. & Choa, V. (2006). Improvement of ultra-soft soil using prefabricated vertical drains. *Geotextiles and Geomembranes*, **24**, No. 6, 339–348.

Deng, Y., Liu, L., Cui, Y. J., Feng, Q., Chen, X. & He, N. (2019). Colloid effect on clogging mechanism of hydraulic reclamation mud improved by vacuum preloading. *Canadian Geotechnica Journal*, **56**, No. 5, 611–620.

Fang, Y., Gou, L. & Huang, J. (2019). Mechanical test on inhomogeneity of dredged fill during vacuum preloading consolidation. *Marine Georesources & Geotechnology*, **37**, No. 8, 1007–1017.

Hansbo, S. (1979). Consolidation of clay by band-shaped prefabricated drains. *Ground Engineering*, **12**, No. 5, 16–25.

Hansbo, S. (1981). Consolidation of fine-grained soils by prefabricated drains. *Proceedings of the 10th International Conference on Soil Mechanics and Foundation Engineering*, Stockholm, Sweden, vol. 3, pp. 677–682.

Hayashi, H., Hatakeyama, O. & Hashimoto, H. (2021). Reducing the secondary consolidation of peat ground using vacuum consolidation. *Proceedings of the Institution of Civil Engineers-Ground Improvement*, **174**, No. 3, 173–184.

Indraratna, B., Rujikiatkamjorn, C. & Sathananthan, I. (2005). Analytical and numerical solutions for a single vertical drain including the effects of vacuum preloading. *Canadian Geotechnical Journal*, **42**, No. 4, 994–1014.

Indraratna, B., Geng, X. & Rujikiatkamjorn, C. (2010). Review of methods of analysis for the use of vacuum preloading and vertical drains for soft clay improvement. *Geomechanics and Geoengineering*, **5**, No. 4, 223–236.

Indraratna, B., Rujikiatkamjorn, C., Balasubramaniam, A. S. & McIntosh, G. (2012). Soft ground improvement via vertical drains and vacuum assisted preloading. *Geotextiles and Geomembranes*, **30**, 16–23.

Kjellman, W. (1952). Consolidation of clay soil by means of atmospheric pressure. In *Proceedings of Conference on Soil Stabilization*. MIT, Boston, MA, USA, pp. 258–263.

Lam, L. G., Bergado, D. T. & Hino, T. (2015). PVD Improvement of soft Bangkok clay with and without vacuum preloading using analytical and numerical analyses. *Geotextiles and Geomembranes*, **43**, No. 6, 547–557.

Lei, H. Y., Hu, Y., Zheng, G., Liu, J. J., Wang, L. & Liu, Y. N. (2019). Improved air booster vacuum preloading method for newly dreged fills: laboratory model study. *Marine Georesources & Geotechnology*, **38**, No. 4, 493–510, https://doi.org/10.1080/1064119X.2019.1599088.

Liu, J., Fu, H., Wang, J., Cai, Y. & Hu, X. (2018). Estimation of influence scope of lateral displacement of soft ground under vacuum pressure with PVD. *Advances in Civil Engineering*, **2018**, https://doi.org/10.1155/2018/8248049.

Long, P. V., Bergado, D. T., Nguyen, L. & Balasubramaniam, A. (2013). Design and performance of soft ground improvement using PVD with and without vacuum consolidation. *Geotechnical Engineering Journal of the SEAGS & AGSSEA*, **44**, No. 4, 36–51.

Long, P. V., Nguyen, L. V., Bergado, D. T. & Balasubramaniam, A. S. (2015). Performance of PVD improved soft ground using vacuum consolidation methods with and without airtight membrane. *Geotextiles and Geomembranes*, **43**, No. 6, 473–483.

Long, P. V., Nguyen, L. V., Tri, T. D. & Balasubramaniam, A. S. (2016). Performance and analyses of thick soft clay deposit improved by PVD with surcharge preloading and vacuum consolidation – a case study at CMIT. *Geotechnical Engineering Journal SEAGS & AGSSEA*, **19**, No. 4, 125–134.

Mesri, G. & Khan, A. Q. (2011). Increase in shear strength due to vacuum preloading. In *Proceedings of the 4th Pan-Am CGS Geotechnical Conference*, Toronto, ON, Canada.

Ni, P., Xu, K., Mei, J. & Zhao, Y. (2019). Effect of vacuum removal on consolidation settlement under a combined vacuum and surcharge preloading. *Geotextiles and Geomembranes*, **47**, No. 1, 12–22.

Ong, C. Y. & Chai, J. C. (2011). Lateral displacement of soft ground under vacuum pressure and surcharge load. *Frontiers of Architecture and Civil Engineering in China*, **5**, No. 2, 239–248.

Phakdimek, S., Ngernbumrung, P. & Soralump, S. (2020). Estimated strength properties of soft clay lump backfilled in a pond improved by vacuum consolidation method. In *The 25th National Convention on Civil Engineering*, Chonburi, Thailand.

Qi, C., Li, R., Gan, F., Zhang, W. & Han, H. (2020). Measurement and simulation on consolidation behaviour of soft foundation improved with prefabricated vertical drains. *International Journal of Geosynthetics and Ground Engineering*, **6**, No. 2, 1–10.

Qiu, Q., Mo, H. H. & Dong, Z. (2007). Vacuum pressure distribution and pore pressure variation in ground improved by vacuum preloading. *Canadian Geotechnical Journal*, **44**, No. 12, 1433–1445.

Robinson, R. G., Indraratna, B. & Rujikiatkamjorn, C. (2012). Final state of soils under vacuum preloading. *Canadian Geotechnical Journal*, **49**, No. 6, 729–739, https://doi.org/10.1139/t2012-024.

Saowapakpiboon, J., Bergado, D. T., Thann, Y. M. & Voottipruex, P. (2009). Assessing the performance of PVD with vacuum and heat preloading. *Geosynthetics International*, **16**, No. 5, 384–392.

Saowapakpiboon, J., Bergado, D. T., Youwai, S., Chai, J. C., Wanthong, P. & Voottipruex, P. (2010a). Measured and predicted performance of prefabricated vertical drains (PVDs) with and without vacuum preloading. *Geotextiles and Geomembranes*, **28**, No. 1, 1–11.

Saowapakpiboon, J., Bergado, D. T., Voottipruex, P., Lam, L. G. & Nakakuma, K. (2010b). PVD Improvement combined with surcharge and vacuum preloading including simulations. *Geotextiles and Geomembranes*, **29**, No. 1, 74–82.

Shang, J. Q., Tang, M. & Miao, Z. (1998). Vacuum preloading consolidation of reclaimed land: a case study. *Canadian Geotechnical Journal*, **35**, No. 5, 740–749.

Shuwang, Y., Xiaowei, F. & Jian, C. (2009). Mechanism of using vacuum preloading method in improving soft clay layers. In *Advances in Ground Improvement: Research to Practice in the United States and China*, Orlando, FL, USA, pp. 308–317.

Tavenas, F., Chapeau, C., Rochelle, P. L. & Roy, M. (1974). Immediate settlements of three test embankments on Champlain clay. *Canadian Geotechnical Journal*, **11**, No. 1, 109–141.

Voottipruex, P., Bergado, D., Lam, L. & Hino, T. (2014). Back-analyses of flow parameters of PVD improved soft Bangkok clay with and without vacuum preloading from settlement data and numerical simulations. *Geotextiles and Geomembranes*, **42**, No. 5, 457–467.

Wang, P., Yu, F., Zhou, Y. & Wang, J. (2019). Effect of a sealed connector on the improvement of dredged slurry under vacuum preloading. *Proceedings of the Institution of Civil Engineers-Geotechnical Engineering*, **173**, No. 3, 254–261.

Wang, P., Han, Y., Zhou, Y., Wang, J., Cai, Y., Xu, F. & Pu, H. (2020). Apparent clogging effect in vacuum-induced consolidation of dredged soil with prefabricated vertical drains (PVDs). *Geotextiles and Geomembranes*, **48**, No. 4, 524–531.

Wu, J., Xuan, Y., Deng, Y., Li, X., Zha, F. & Zhou, A. (2020). Combined vacuum and surcharge preloading method to improve Lianyungang soft marine clay for embankment widening project: a case. *Geotextiles and Geomembranes*, **49**, No. 2, 452–465.

Xu, B. H., He, N., Jiang, Y. B., Zhou, Y. Z. & Zhan, X. J. (2020). Experimental study on the clogging effect of dredged fill surrounding the PVD under vacuum preloading. *Geotextiles and Geomembranes*, **48**, No. 5, 614–624, https://doi.org/10.1016/j.geotexmem.2020.03007.

Zhang, D., Fu, H., Wang, J., Zhu, D., Hu, D., Hu, X., Du, Y., Gou, C., Wang, C., Li, M. & Wu, H. (2021). Behaviour of thick marine deposits subjected to vacuum combined with surcharge preloading. *Marine Georesources & Geotechnology*, **39**, No. 10, 1147–1156.

Zhou, Y., Wang, P., Shi, L., Cai, Y. & Wang, J. (2021). Analytical solution on vacuum consolidation of dredged slurry considering clogging effects. *Geotextiles and Geomembranes*, **49**, No. 3, 842–851, https://doi.org/10.1016/j.geotextmem.2020.12.013.

**The Editor welcomes discussion on all papers published in Geosynthetics International. Please email your contribution to discussion@geosynthetics-international.com**